

Article

Potential of Alternative Organic Binders in Briquetting and Enhancing Residue Recycling in the Steel Industry

Elsayed Mousa ^{1,2,*} , Hesham Ahmed ^{2,3}  and Daniel Söderström ⁴¹ SWERIM AB, Aronstorpsvägen 1, 974 37 Luleå, Sweden² Central Metallurgical Research and Development Institute (CMRDI), Cairo 12422, Egypt; hesham.ahmed@ltu.se³ MiMeR, Luleå University of Technology, 971 87 Luleå, Sweden⁴ Formerly at SSAB EMEA AB, 971 88 Luleå, Sweden; danne.soder@telia.com

* Correspondence: elsayed.mousa@swerim.se

Abstract: Steel production generates various types of residues that cannot be directly recycled in the production process without pre-treatment and agglomeration. In the present study, recipes were designed to develop briquettes in a blast furnace (BF) with the partial replacement of cement with alternative commercial organic binders, including molasses–lime, bitumen, keracoal, carboxymethyl cellulose, and wood tar. The briquettes were produced using a technical-scale vibrating machine and the mechanical strength was evaluated using drop test and standard tumbler index results. The reduction behaviour was investigated by thermogravimetric analysis (TGA) coupled with QMS. A heat and mass balance model (MASMOD) was used to evaluate the potential of developed briquettes to reduce the energy consumption and CO₂ emissions from the BF. Although cement was superior in developing mechanical strength, bitumen was the best among the other alternative organic binders and provided sufficient strength to the briquettes at 2.0% addition, which corresponded to 18.2% replacement of total cement. The briquettes containing bitumen possessed a higher reduction rate and lower activation energy compared to cement. The MASMOD calculation demonstrated that the developed briquettes have the potential to provide annual savings of 15,000–45,000 tons of lump coke, 4500–19,500 tons of CO₂ emissions, and 5000–20,000 tons of limestone in Swedish BFs.

Keywords: blast furnace; recycling; residues; organic binders; reduction; modelling; CO₂ emission



Citation: Mousa, E.; Ahmed, H.; Söderström, D. Potential of Alternative Organic Binders in Briquetting and Enhancing Residue Recycling in the Steel Industry. *Recycling* **2022**, *7*, 21. <https://doi.org/10.3390/recycling7020021>

Academic Editor: Daniel Goldmann

Received: 16 February 2022

Accepted: 17 March 2022

Published: 1 April 2022

Publisher's Note: MDPI stays neutral with regard to jurisdictional claims in published maps and institutional affiliations.



Copyright: © 2022 by the authors. Licensee MDPI, Basel, Switzerland. This article is an open access article distributed under the terms and conditions of the Creative Commons Attribution (CC BY) license (<https://creativecommons.org/licenses/by/4.0/>).

1. Introduction

Iron and steel manufacturing is associated with the generation of by-products and residues that are unusable without pre-treatment and agglomeration. Environmental legislation and material costs are two of the vital factors in recycling these materials and recovering their associated minerals to the greatest extent possible. The recycling process is not only able to save virgin raw materials, but it can also reduce disposal costs and protect the environment from hazardous materials. According to the World Steel Association [1], the steel industry is paying more attention to adopting a circular economy model that aims to reach zero waste through the reuse and recycling of all by-products. The aim is to find new markets and applications for steel by-products and waste materials, such as slag, dust, and sludge. The average quantities of generated dust, fines, sludge, and scales in integrated steel plants are in the range of 60–150 kg per ton of steel, which corresponds to approximately 3–7.5% of the total iron [2]. These fines cannot be directly charged back into the BF or steelmaking unit without conducting proper sorting, mixing, and agglomeration processes. Agglomeration via sintering and briquetting processes plays a vital role in the internal recycling of by-products to recover iron, carbon, and lime.

The traditional and most common way to recycle these residues back to the BF is via a sintering plant or by pelletizing; however, BFs in Nordic countries (Sweden and Finland) operate on 100% pellets [3], and the recycling of steel mill residues takes place

using cement-bonded briquettes [4,5]. The briquettes must have sufficient mechanical strength for handling, transportation, and charging into the BF. The selection of residue blends and pre-treatment and mixing of the residues are essential steps to achieve uniform quality mixtures for briquetting [5–7]. The selection of residues is based on availability and the chemical, physical, and mineralogical composition [8]. A binder is required to give the proper mechanical strength for handling, transportation, storage, and top charging into the BF [9–11]. The briquette binder plays a key role in the process of briquette production in terms of the cold strength, thermal stability, chemical composition, and cost. Portland cement is the most common binder used in the briquetting of steel mill residues to form cold-bonded briquettes [11,12], due to its availability, its ability to develop strength at room temperature, and its chemical composition, with lime contributing to the slag formation. In addition, cement as binder is available at acceptable costs, has a neutral effect on BF reactions, and can increase the mechanical strength of the briquettes [13]. With increased cement content, the cold compression strength of the briquettes will be increased [7,14] if the acicular structure of the ettringite phase is formed during hydration [15]. The ettringite needles grow over time, forming a network between cement particles and contributing to the briquette strength via the formation of calcium silicate hydrates (C-S-H). Upon heating the briquettes, the C-S-H is decomposed at 500–700 °C and, consequently, the briquettes lose their strength and may disintegrate into finer fractions [16] unless there is another phase formed that can contribute to the strength. Although the mechanical strength of the cold-bonded briquettes increases by increasing the cement ratio in the mixture, the slag generation and the bonded water entering the BF with the briquettes will also increase [13]. It has been stated that using 10% iron ore burden material in the form of cement-bonded briquettes, which contain about 10% cement, will increase the slag generation by about 15 kg/tHM. In addition, the cement industry contributes to fossil CO₂ emissions at a rate of 800 kg CO₂ per ton of product cement, which represents about 7% of the total world CO₂ emissions [8]. Biomass lignin has been used for partial replacement of cement in BF briquettes [3]. The replacement of up to 25% of cement with lignin resulted in adequate cold mechanical strength for the briquettes and a faster reduction rate; however, the briquettes' strength was significantly reduced after reduction, which was attributed to the dehydration of cement and the gasification of lignin. When embedding torrefied and pelletized sawdust in the briquetting mixture, more cement was needed to obtain proper mechanical strength for implementation in the BF, as discussed elsewhere [17,18]. In a recent study by the authors [19], organic binders showed promising results in developing biocarbon briquettes for metallurgical applications; however, they have not been tested for the briquetting of steel mill residues. Research on the utilization of traditional organic binders in top-charged agglomerates in iron manufacturing BFs is very limited.

In this paper, the authors explore and study the possibility of the partial replacement of traditional cement by alternative commercial organic binders. BF briquettes are developed that enable the recirculation of unexploited residues in the steel plant to be increased. The developed agglomerates are evaluated in terms of their mechanical strength, reduction behaviour and overall impact on BF efficiency using a static heat and mass balance-based model (MASMOD).

2. Materials and Methods

2.1. Materials Selection and Analysis

The residues that were used to manufacture the briquettes were provided by SSAB. The chemical analysis of the applied materials is provided in Table 1. The pre-mixture (pre-mix) consists of fine-grained scrap, LD sludge, briquette fines, and filter dust mixed in specific proportions to meet the physical and chemical characteristics for BF implementation. The alternative commercial organic binders that have been selected for this study are: molasses, hydrated lime, keracoal, bitumen, carboxymethyl cellulose (CMC) and wood tar. The moisture content was measured for all binders before mixing with the steel mill residues, as shown in Table 2. The binder addition was calculated on a dry weight basis.

Table 1. Chemical analysis of applied materials.

	Pre-Mix.	BF Dust	Coke Fines	Cement
	wt.%, Dry Basis			
Fe	46.41	23.80	0.35	2.46
CaO	22.85	14.74	0.05	65.00
SiO ₂	5.16	6.84	7.19	20.10
MnO	1.31	0.44	0	0.04
P ₂ O ₅	0.15	0.08	0.03	0.10
Al ₂ O ₃	2.18	2.21	3.12	3.47
MgO	2.55	1.65	0.07	2.11
Na ₂ O	0.06	0.06	0.05	0.17
K ₂ O	0.02	0.03	0.16	0.93
V ₂ O ₅	1.2	0.39	0.01	0.02
TiO ₂	0.85	0.37	0.18	0.21
Cr ₂ O ₃	0.12	0.04	0	0.03
GLF	2.9	-39.0	-	-
C	5.9	33.53	87.86	0.70
S	0.73	0.63	0.56	1.37
Moisture	11.13	0.30	9.98	0.00

Table 2. Moisture content in the applied binders.

Material	Molasses	Hydrated Lime	Keracoal	Bitumen	CMC	Wood Tar
Moisture, wt.%	3.64	4.82	2.53	9.97	6.94	2.26

2.2. Recipe Design

The approach adopted to design the recipes in this study consists of 3 steps, as summarized in Table 3 and described as follows:

2.2.1. Design of Recipes R0–R3

In this step, reference recipe R0 was designed to simulate a standard recipe at a briquetting plant. In recipes R1–R3, 4 wt.% of the traditional binder cement in coke fines-free briquettes was replaced with one of the alternative selected binders. The 4 wt.% of cement replacement in the briquettes corresponds to 36.36 wt.% of the total added cement.

2.2.2. Design of Recipes R4–R8

In this step, reference recipe R4 was designed to simulate the standard recipe (R0) but with the addition of 5 wt.% coke fines. Recipes R5–R8 were designed to be similar to R4 in composition but with different binders. In R5–R7, 4 wt.% of cement was replaced with 4 wt.% of alternative binders while, in R8, 4 wt.% of cement was replaced by only 1 wt.% of CMC (carboxymethyl cellulose).

2.2.3. Design of Recipes R9–R15

In this step, reference recipe R9 was designed to simulate the standard recipe (R0) but with the addition of only 9 wt.% of cement instead of 11 wt.%. In addition, recipes R10, R11 and R14 were designed using 9 wt.% of cement and 2 wt.% of alternative binders without the addition of coke fines. On the other hand, R12, R13 and R15 were designed

with the addition of 5 wt.% coke fines. The 2.0 wt.% replacement of cement in the briquettes corresponds with the 18.2 wt.% of cement added in the briquette.

2.3. Technical Scale Briquetting

The briquettes were produced using a Teksam VU600/6 briquetting machine. The machine consisted of a hydraulic station and a press that reached up to 100 bars. The mould was installed on the vibrating station to improve and enhance the compaction of the materials. The briquetting process was started by weighing the materials and adjusting the proportions according to the recipes in Table 3. A batch with a total weight of ~25 kg/recipe was prepared. The materials were mixed well using a SoRoTo 40 L-33 cement mixer with several impellers. The water was gradually added until the mixture started to form a homogeneous slurry. The prepared mixture was fed into the steel moulds of the briquetting machine with 16 hexagonal holes. After filling the mould with the materials, vibration was applied for ~30 s accompanied by mechanical pressing force to push the briquettes out. The briquettes with hexagonal shape (height ~7.0 cm, edge 3.3 cm) were placed on a wooden pallet and then cured in humidified atmosphere for 24 h. After curing, the briquettes were left to dry at ambient temperature for 28 days. The mechanical strength was initially evaluated based on the drop test. Each briquette was dropped on a metal plate from a distance of 1.0 m. The maximum number of drops was fixed at 50 drops or until the briquette had reached almost half of its height. Based on the conducted drop test, some recipes were selected to measure the tumbler index (TTH) according to the Swedish standard SS-ISO 3271:2007. In this case, ~15 kg of briquettes from each recipe was charged to the tumbler device after drying for up to 4 weeks. The tumbler was a rotating drum with a diameter of ~90 cm and rotation speed of 25 rpm. The tumbling time was fixed at 8 min (200 revolutions). The fractions that were bigger than 6.0 mm were weighed after tumbling and given as a percentage of the initial charged weight of the briquettes.

Table 3. Design and expected benefits of BF briquettes.

Stage No.	Recipe No.	Pre-Mix	BF Dust	Coke Fines	Cement	Molasses/Lime	Keracoal	Bitumen	CMC	Wood Tar	Total wt.%
Stage 1	R0	79	10	0	11	0	0	0	0	0	100
	R1	79	10	0	7	2.7/1.3	0	0	0	0	100
	R2	79	10	0	7	0	4	0	0	0	100
	R3	79	10	0	7	0	0	4	0	0	100
Stage 2	R4	74	10	5	11	0	0	0	0	0	100
	R5	74	10	5	7	2.7/1.3	0	0	0	0	100
	R6	74	10	5	7	0	4	0	0	0	100
	R7	74	10	5	7	0	0	4	0	0	100
	R8	77	10	5	7	0	0	0	1	0	100
Stage 3	R9	81	10	0	9	0	0	0	0	0	100
	R10	79	10	0	9	1.3/0.7	0	0	0	0	100
	R11	79	10	0	9	0	0	2	0	0	100
	R12	74	10	5	9	1.3/0.7	0	0	0	0	100
	R13	74	10	5	9	0	0	2	0	0	100
	R14	79	10	0	9	0	0	0	0	2	100
	R15	74	10	5	9	0	0	0	0	2	100

3. Results and Discussion

3.1. Mechanical Strength

The number of drops that each briquette was able to hold after drying for 28 days is shown in Figure 1. The shapes of some of the selected briquettes subjected to the drop test after drying for 7 and 28 days are shown in Figure 2. Cement was superior for briquette strength. Most of the briquettes prepared by replacing 4 wt.% of cement with alternative binders (R1–R3 and R5–R8) were weak and were not able to reach 50 drops without being severely damaged. By reducing the replacement ratio of cement to 2 wt.% with alternative organic binders, the briquettes with bitumen (R11 and R13) were able to reach to 50 drops

while the rest of the recipes showed a low number of drops. Figure 3 shows the weight loss during the drop test of the briquettes. It can be seen that among the different types of tested binders, only R11 and R13 (produced by 2 wt.% replacement of cement with bitumen) were able to achieve a high number of drops with low fine generation.

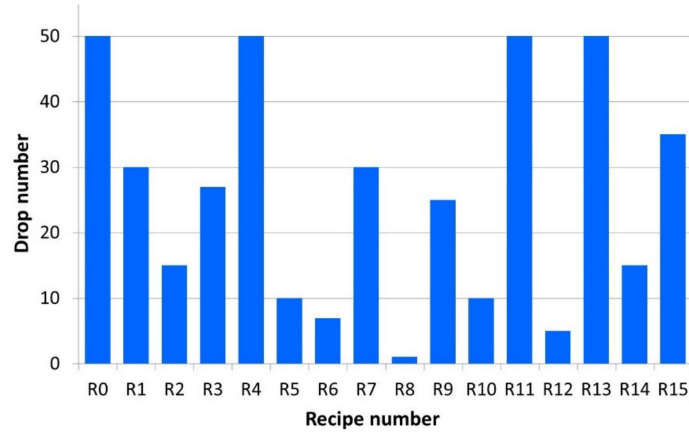


Figure 1. Drop test for the developed briquettes.

Recipe No.	Briquette before drop test	After 7 days of curing	After 28 days of curing
R0			
R4			
R10			
R11			
R13			
R15			

Figure 2. Photomicrograph of the briquettes after drop test.

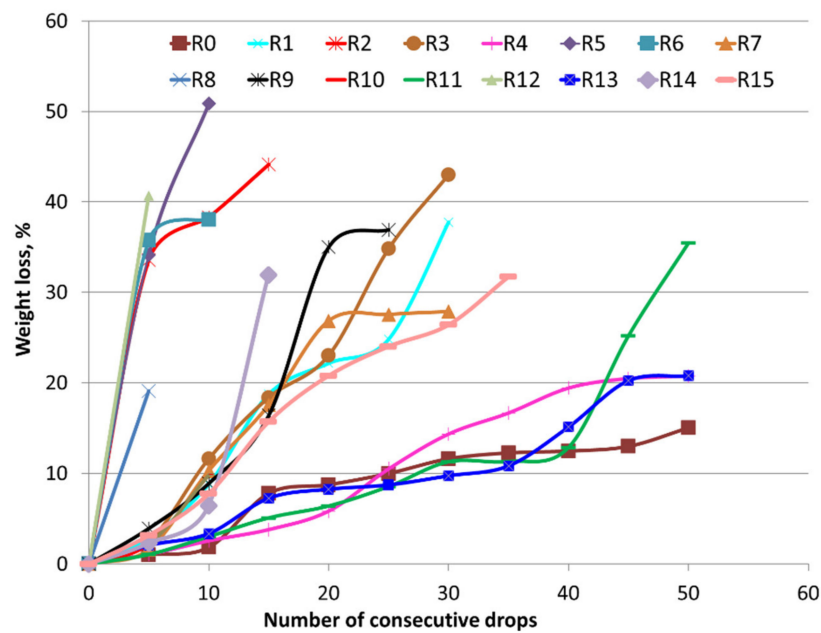


Figure 3. Weight loss during the drop test of different briquettes.

Based on the design concept of the recipes and on the results of the drop test, recipes R0, R10, R11, R13 and R15 were chosen for measuring the tumbler index after a curing time of about 28 days. The criteria of selection can be clarified as follows: (1) R0 is selected as a reference without alternative binders; (2) R10 is selected to verify the results of the drop test using the standard tumbler index and is compared with R11 (both recipes were designed without coke breeze); and (3) R15 is selected for comparison with R13 (both recipes were designed with 5% coke breeze at the same level of binder ratio). The resulting tumbler index and the shape of the briquettes after the tumbler test are given in Figures 4 and 5, respectively. Recipes R0, R11, and R13 demonstrate very good strength with TTH equal to 77.2%, 74.8%, and 68.1%, respectively. On the other hand, R10 (2 wt.% cement replaced with molasses/lime) and R15 (2.0 wt.% cement replaced with 2.0 wt.% wood tar) were weak, with TTH equal to 25.0% and 36.7%, respectively. This indicates that cement can be replaced with bitumen up to 2.0 wt.% without impairing briquette strength, while other types of tested alternative binders deteriorated the briquettes’ strength and were not able to achieve the minimum level of TTH ($\geq 60\%$) for the blast furnace.

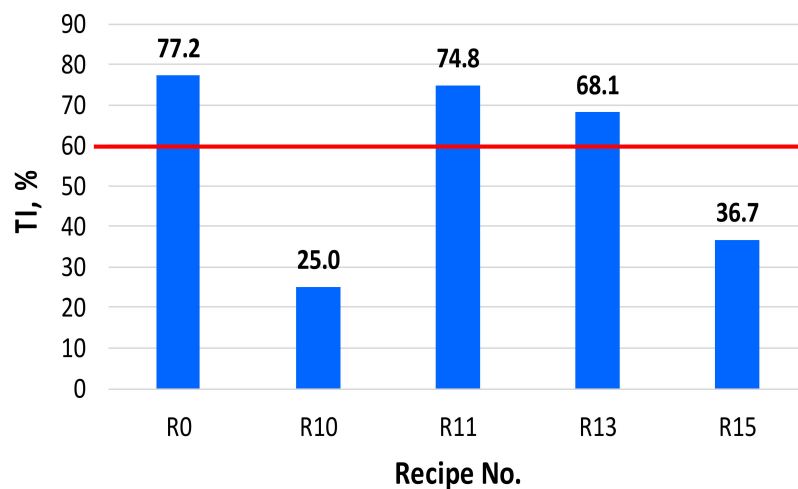


Figure 4. Tumbler index of reference and developed briquettes; the red line represents the minimum accepted level of TTH for the blast furnace.

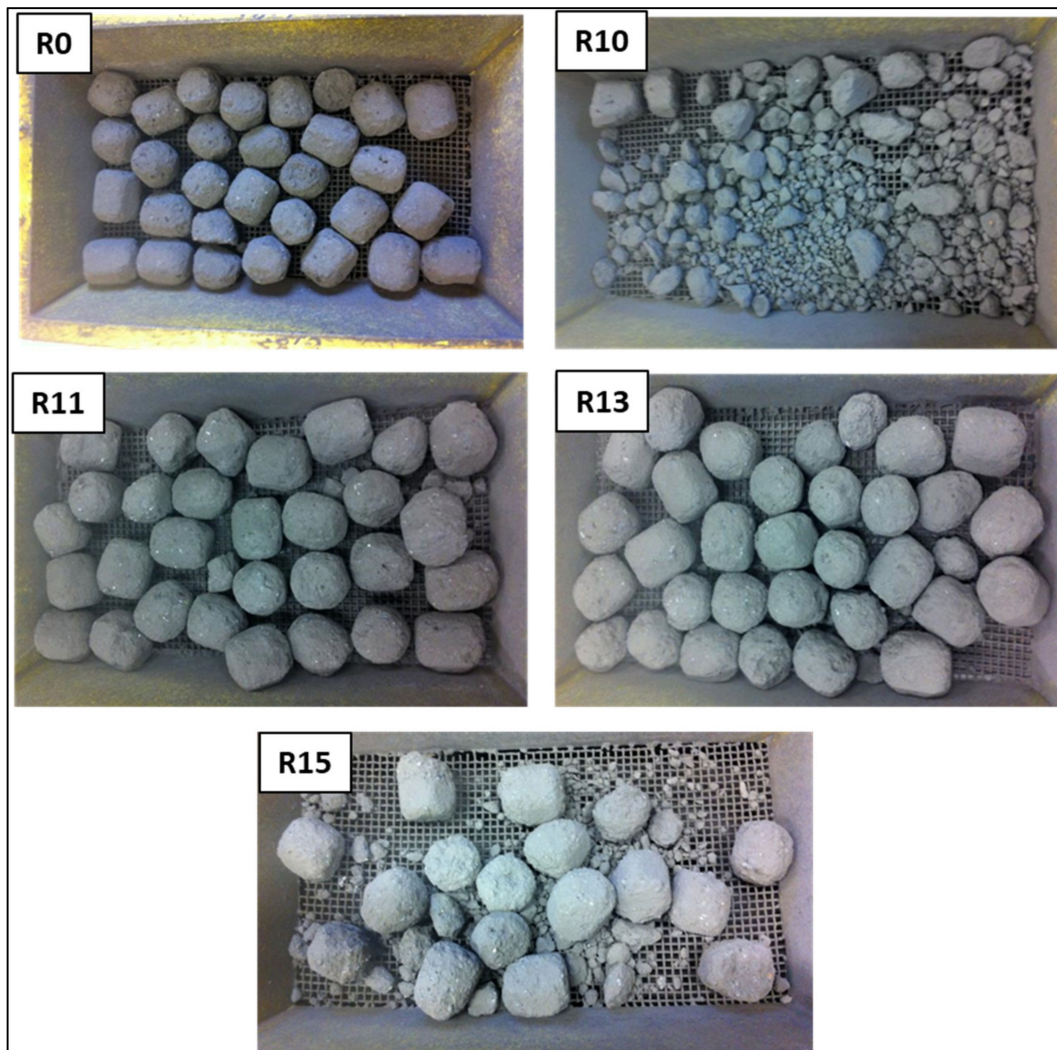


Figure 5. Briquettes after tumbler index.

3.2. Reduction Behaviour

In addition to the reference briquette, three recipes (R11, R13 and R15) were chosen for the reduction. All recipes achieved the target of mechanical strength ($TTH \geq 50\%$) except R11 ($TTH = 34\%$), which was selected because it was closer to the target ($TTH \geq 50$) compared to R10 ($TTH = 25\%$). Briquettes from the selected recipes were subjected to reduction in a thermogravimetric analyser (TGA) in Ar atmosphere under the blast-furnace-simulated thermal profile. The produced gases were identified using quadruple mass spectroscopy (QMS).

Figure 6 shows the mass loss curves as a function of time and temperature. It can be seen that, in all cases, ~ 5 wt.% of original weight was lost at temperatures lower than 600 °C, which can be attributed to the evaporation of mechanical and chemical combined water and release of contained volatiles. As the temperature increased, the briquettes showed different rates of weight loss. For the reference briquette, the weight remained stable up to ~ 750 °C, while other samples manifested a weight loss, with the highest mass loss in the case of R11. R13 and R15 showed similar behaviour up to ~ 880 °C. The mass loss rate for sample R11 was always higher at or above 600 °C and the net mass loss was ~ 26.6 wt.%. Although the mass loss for the alternative binders containing briquettes (R13 and R15) at a given time and temperature was higher compared to the reference briquette, the later mass loss curve crossed their mass loss curves at and above ~ 860 °C. The mass loss rate for R0 remained the second highest until the reaction was completed, with a net

mass loss of ~23.8 wt.%. Above ~880 °C, the mass loss rate for R13 increased compared to that of R15, with a net mass loss of 21.1 wt.% in the case of R13 and 18.3 wt.% in the case of R15.

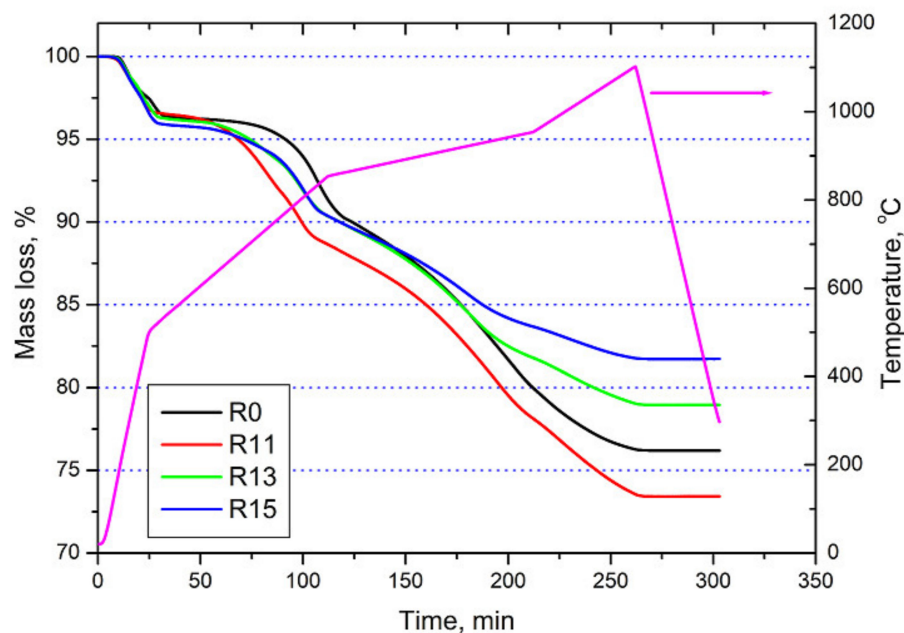
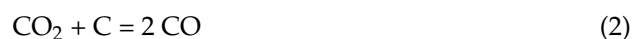


Figure 6. Mass loss curves of studied briquettes as a function of time and temperature.

The off-gas analysis during the conducted experiments showed that all samples released H₂O at low temperature (up to 600 °C), which explains the early mass loss detected by TGA. In addition to the detected H₂O, alternative binders containing briquettes released hydrocarbons in the same temperature range. Above 600 °C, the only detected gases were CO₂ and CO, which are the product gas of the following reactions:



Looking at the rate of mass loss curves (DTG) given in Figure 7, it is obvious that the reaction proceeds through consecutive series of reactions. Early reactions, below 600 °C, were due to water evaporation and the release of hydrocarbons, in which no significant difference was detected between all samples. As the temperature increased, a peak was detected at ~750 °C. The intensity was highest for R11, which can be explained by the interaction between bitumen and reducible oxygen in the briquette. For R13, the peak intensity was lower than that of R11 despite containing the same binder. This difference can be attributed to the lower amount of available reducible oxygen (R13 contains 84 wt.% residue compared to 89 wt.% in R11). The second peak for all the samples except the reference sample appears at ~805 °C, which is probably due to the reactive carbon-containing binder that reacts with internally generated carbon dioxide. For the reference sample, this peak appeared at approximately 850 °C. Later, when the temperature approached ~920 °C, the DTG curves for R15 and R13 showed a peak. A similar peak but higher in intensity (higher mass loss rate) appeared later at ~940 and ~950 °C for R11 and R0, respectively. This difference can be attributed to the presence of reactive coke fines, which reacted with either locally generated CO₂ or reducible oxygen.

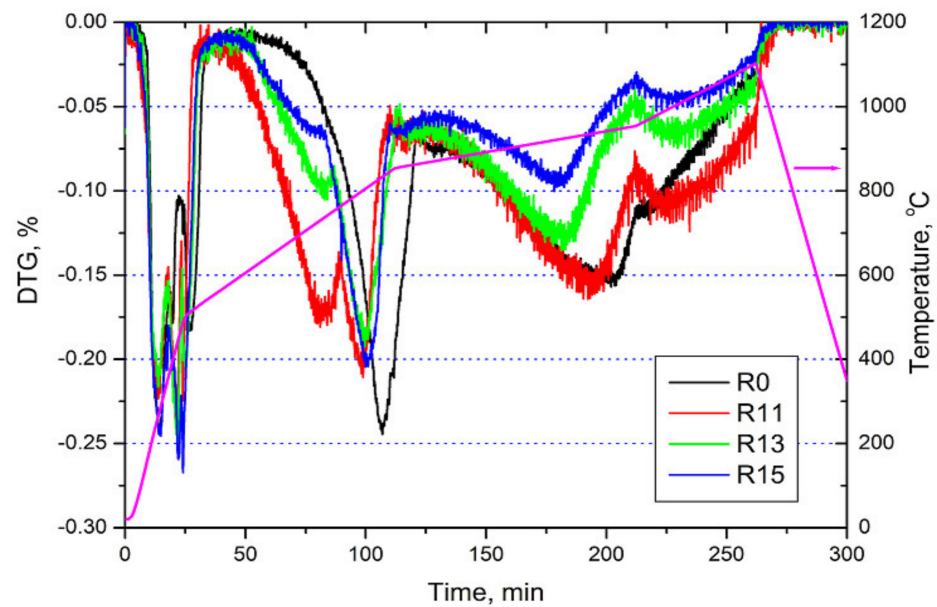


Figure 7. The first derivative (DTG) of the mass loss curves as a function of time and temperature.

The difference in the net mass loss can be explained by either the available reducible oxygen (see Tables 1 and 4) or the improved carbon utilization efficiency. The latter can be visualized due to the fact that shifting the reduction of FeO to Fe toward lower temperature will result in less carbon consumption and higher utilization of CO [20,21]. The latter suggestion can be justified by the DTG results. It is evident that the DTG peaks (which correspond to different reactions) shift toward lower temperature when an alternative binder is being used. Starting from lower temperature, they have been found to be in the following order: R15 < R13 < R11 < R0.

Table 4. The peaks temperature and the corresponding reactions.

Sample	Peak Temperature	Expected Corresponding Reaction
All samples	Below 600 °C	Water evaporation and release of volatiles
R11, 13 and 15	~750 °C	Hematite—wüstite
R0	~805 °C	Hematite—wüstite
R13 and R15	~920 °C	Wüstite—metallic iron
R11	~940 °C	Wüstite—metallic iron
R0	~950 °C	Wüstite—metallic iron

Table 4 shows the different peak temperatures (as seen in Figure 7), the corresponding temperatures and the speculated reactions. The carbothermic reduction of iron oxide under atmospheric pressure is known to proceed through the gas–solid reaction between locally generated CO and iron oxide particles. The reduction gaseous products are either CO or CO₂ or most likely a combination of both depending on the temperature. If the gas product is only CO₂, this means minimum mass loss (less carbon consumed) to achieve complete reduction. If the gas product is only CO, this means maximum mass loss (high carbon is being consumed) to achieve complete reduction. Table 5 shows the C/O molar ratio in each briquette and the minimum and maximum theoretical mass loss, taking into account the early mass loss until 600 °C, compared with the actual mass loss.

Table 5. C/O molar ratio, minimum and maximum mass loss and the experimental mass loss.

Sample	C/O Molar Ratio	Minimum Mass Loss	Maximum Mass Loss	Actual Mass Loss
R0	0.6	29.9	38.0 *	23.8
R11	1.1	21.9	27.8	26.6
R13	1.8	20.1	25.6	21.1
R15	1.2	23.9	30.4	18.3

* there is enough carbon to complete the reduction.

The experimental mass loss should lie between the maximum and the minimum values of mass loss. When the experimental mass loss was very close to the minimum value, this means that the gaseous reaction product was dominated by CO₂. This indicates that the reduction of wüstite was shifted toward lower temperature and higher CO utilization, which results in less carbon consumption. In some cases, the experimental mass loss is even lower than the calculated minimum mass loss, which means that the reduction is not complete or some of the input iron oxide was in a lower oxidation state than hematite.

The reduction kinetics and apparent activation energy values of the magnetite–wüstite and wüstite–metallic iron steps were further calculated by means of the Arrhenius equation (Equation (3)), assuming a first order reaction.

$$k = \frac{1}{w_c} \frac{dw_c}{dt} = k^0 e^{-\frac{E_a}{RT}} \quad (3)$$

where w_c is the initial mass of carbon, k^0 is the pre-exponential factor, E_a is activation energy, R is the universal gas constant and T is the absolute temperature. Equation (3) is valid for isothermal experiments. In the present investigation, the carbothermic reduction of iron oxide was conducted non-isothermally. It was taken into account that the slow non-isothermal heating cycle consists of an infinite number of discrete isothermal sections. Based on this concept, the mass loss curves (see Figure 6) were discretized into small segments where the difference in temperature is very small. The kinetic parameters k^0 and E_a can be estimated by plotting the logarithmic k vs. the reciprocal of absolute temperature (Equation (4)).

$$\ln(k) = \ln(k^0) - \frac{E_a}{RT} \quad (4)$$

The slope of the obtained line is $-\frac{E_a}{R}$ and the intercept with the x -axis is k^0 ; however, only E_a is presented here. The estimated apparent activation energies of iron oxide reduction are given in Table 6.

Table 6. The estimated apparent activation energies for different iron oxide reduction steps.

Recipe No	Step	Equation of Linear Regression	R ²	Activation Energy, kJ/mol
R0	Magnetite–wüstite	$y = -18182x + 9.3913$	0.97	151
	Wüstite–metallic iron	$y = -31276x + 19.717$	0.97	260
R11	Magnetite–wüstite	$y = -15707x + 7.1346$	0.97	130
	Wüstite–metallic iron	$y = -21954x + 12.718$	0.96	182
R13	Magnetite–wüstite	$y = -12066x + 2.8546$	0.96	100
	Wüstite–metallic iron	$y = -25308x + 15.343$	0.97	210
R15	Magnetite–wüstite	$y = -9908.9x + 0.4331$	0.90	82
	Wüstite–metallic iron	$y = -23845x + 13.949$	0.98	198

All estimated activation energy values are well above the activation energy of diffusion-controlled reactions at ~40 kJ/mol. The high activation energy values indicate that the reduction is controlled by the chemical reaction. It can also be seen that the estimated values for all alternative binder-containing briquettes were always lower than those for the

reference briquette. Moreover, the activation energy values estimated for the magnetite–wüstite conversion step were always lower than those of the wüstite–metallic iron step. Interestingly, the values calculated for the wüstite–metallic iron step are very close to the earlier calculated values for the gasification of carbon under similar conditions [22]. This indicates that, under the present experimental conditions, carbon gasification (Equation (2)) is the rate-limiting reaction during carbothermic reduction of wüstite.

3.3. Heat and Mass Balance Calculations (MASMOD)

The potential benefits of using alternative organic binders for partial replacement of cement have been evaluated using the heat and mass balance model (MASMOD). The MASMOD is a numerical one-dimensional model, which is based on the thermodynamic equilibrium of reactions that take place in the BF [23]. The model iterates heat and mass balances within the furnace based on input data. These inputs are converted to units/ton of hot metal (tHM), which is corrected with the efficiency of the specific BF as well as thermodynamic equilibrium data. The principle of MASMOD is schematically described in Figure 8 [23]. As can be seen, the BF is divided into an upper and a lower zone connected via the thermal reserve zone using the equilibrium between CO/CO₂ and H₂/H₂O in the gas and Fe/FeO in the burden.

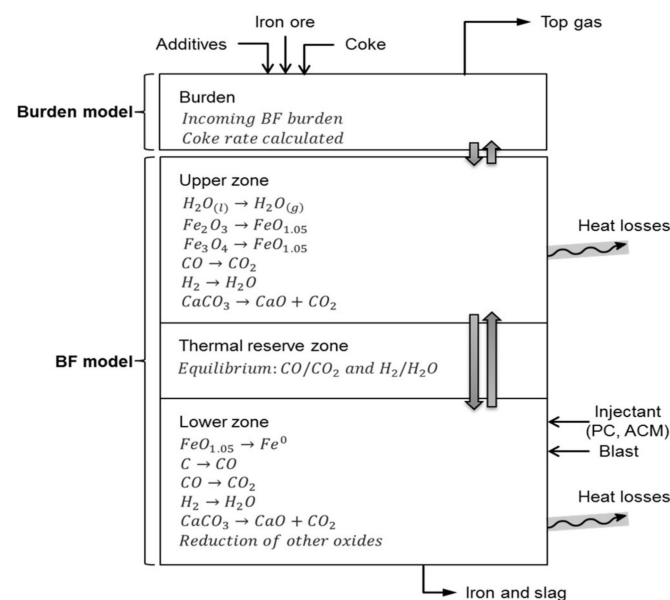


Figure 8. Blast furnace model, after [23].

Four recipes have been selected for evaluation: R0 (ref.), R11 (2 wt.% bitumen), R13 (2 wt.% bitumen + 5 wt.% coke fines) and R15 (2 wt.% wood tar + 5 wt.% coke fines). Those recipes, except for R15, exhibited good mechanical strength to be applied in BF. The following assumptions were made:

- The production rate of hot metal (tHM/h) was kept constant;
- RAFT (Raceway adiabatic flame temperature) was kept constant while TRZT (thermal reserve zone temperature) and top gas temperature were varied;
- Shaft efficiency was assumed to be constant as the reference;
- Slag basicity was kept the same by adjusting the amount of limestone charged to BF, while the slag rate varied;
- PCI (pulverized coal injection) was kept constant, while coke rate was allowed to vary;
- Briquette rate was kept constant at 102.1 kg/tHM, while the pellets rate was allowed to vary to keep the production rate constant;
- The generated dust and sludge were kept constant at 15 kg/tHM of dust and 5.0 kg/tHM for sludge.

On the basis of the above assumption and modelling approach, the operation parameters of one of the Swedish BFs are given in Table 7. Chemical analysis of the investigated briquettes that were used in MASMOD is given in Table 8. Besides the effect of the binders on the analysis of the briquettes, the pre-mix used in the briquettes was collected from the plant during different periods, which could also affect the briquette analysis. The changing of the burden content by charging the developed briquettes (R11, R13 and R15) compared to the reference (R0) can be seen in Figure 9. The rate of olivine-fluxed pellets (MBPO) per ton of hot metal was increased, while limestone and coke rate were decreased by different rates. The coke consumption was decreased by ~4, ~12, and ~7 kg/tHM by charging the developed briquettes R11, R13, and R15, respectively. The increase in pellets rate is attributed to the lower content of iron in the developed briquettes compared to the reference, while the higher CaO and carbon content in the developed briquettes contribute to reducing the coke consumption. The amount of input carbon from different charged burden materials is given in Figure 10. It can be seen that the total input carbon content is almost constant in all cases at 396 kg/tHM. The developed briquettes contribute more carbon to the process than standard briquettes, which consequently reduces the required lump coke. Figure 11 shows the changing of coke and CO₂ emission by using the developed briquettes. The developed briquettes R13 showed the highest coke saving of 3.8 wt.% less coke compared to the reference briquettes, followed by R15 with 2.16 wt.%, and lastly, R11 with 1.28 wt.%, which corresponds directly to the carbon content in the briquettes (R13 > R15 > R11), as given in Table 8. On the other hand, the highest mitigation of CO₂ emission is exhibited by R13 (0.4 wt.% of CO₂ less than the reference), followed by R11 (0.34 wt.% less than reference), and lastly, R15 (0.09 wt.% less than reference). This corresponds directly to the charging rate of limestone, which is added to adjust the basicity. As can be seen in Figure 9, all developed recipes are accompanied by lower limestone addition compared to the reference and, among developed recipes, R13 showed the lowest charging rate of limestone, while R15 showed the highest charging rate.

Table 7. Set-up parameters for MASMOD.

Parameter	Unit	Values in Blast Furnace	Limits
Feed and Production Rate			
Coke	kg/tHM	314.5	Variable
PCI	kg/tHM	143.0	Kept constant
Limestone	kg/tHM	18.4	Varies to adjust the slag basicity
Pellets	kg/tHM	1321.8	Varies to keep the production constant
LD slag	kg/tHM	45.1	Kept constant
Injected dust	kg/tHM	6.1	Kept constant
Briquettes	kg/tHM	102.1	Kept constant
Production rate	tHM/h	275.3	Kept constant
Operating conditions			
Eta CO	%	54.9	Varies
Eta H ₂	%	35.5	Constant as reference
Top gas temperature	°C	131.7	Varies
Shaft efficiency	%	92.7	Kept constant
Blast temperature	°C	1076	Kept constant
TRZT	°C	850	Varies
O ₂ in the blast	%	4.17	Kept constant
RAFT	°C	2161	Kept constant
Heat losses	MJ/tHM	353.1	Kept constant
Heat loss distribution	%	55.2	Kept constant

Table 8. Chemical composition of reference and developed briquettes.

Component, wt.%	Recipe No.			
	R0	R11	R13	R15
CaO	17.94	21.46	21.40	18.88
MgO	1.69	2.06	1.96	2.00
SiO ₂	5.66	6.74	6.91	6.16
Al ₂ O ₃	1.69	1.91	2.13	1.99
TiO ₂	0.43	0.51	0.49	0.47
V ₂ O ₅	0.63	0.74	0.62	0.63
Na ₂ O	0.06	0.07	0.07	0.07
K ₂ O	0.09	0.13	0.13	0.12
S	0.56	0.79	0.88	0.64
P	0.04	0.05	0.04	0.04
Mn	0.72	0.73	0.627	0.658
Fe	50.71	37.06	34.09	40.49
C	9.21	12.65	19.60	15.20
Zn	0.07	0.07	0.07	0.07
Cr	0.05	0.07	0.05	0.05
Moisture	3.69	2.55	3.00	2.63

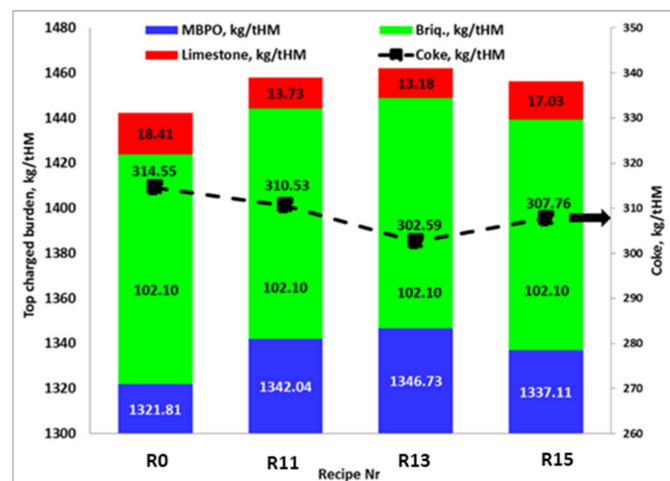


Figure 9. Charged burden to BF at different types of briquettes.

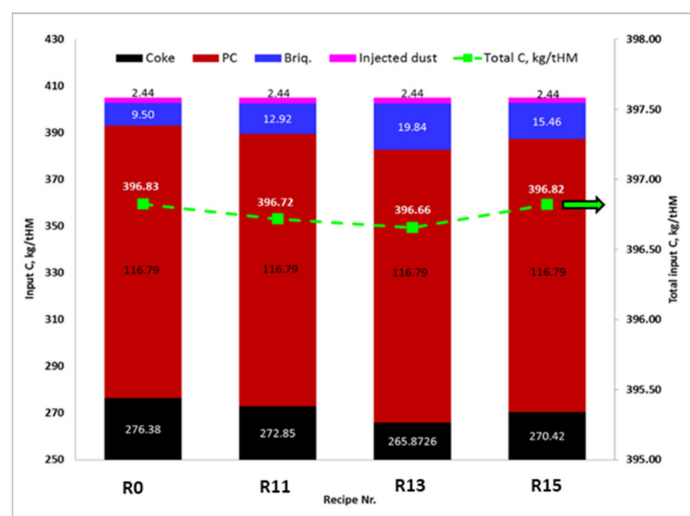


Figure 10. Source of input carbon from different charged materials.

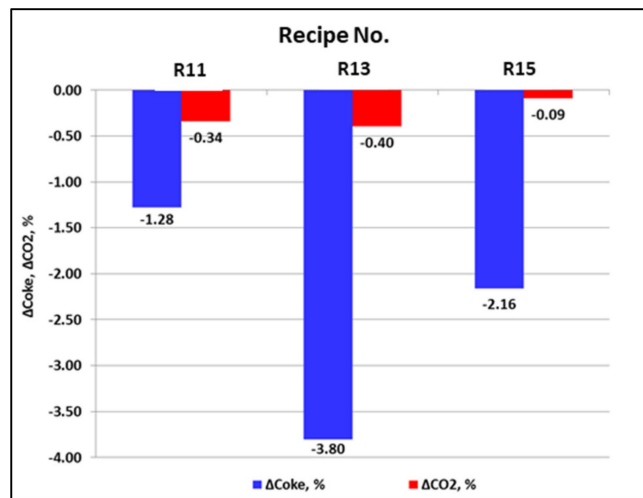


Figure 11. Changing of coke and CO₂ emissions at different cases of developed briquettes.

Assuming that the three BFs in Sweden are operating with full annual production of 3.8 million tHM, the replacing of standard briquettes with the developed briquettes R11, R13 and R15 is able to annually save ~15,000 tons, ~45,000 tons and 26,000 tons of lump coke, respectively, as shown in Figure 12. The consumption of limestone will be reduced by 5000–20,000 tons per year. The CO₂ emission from the three BFs will be decreased by an equivalent of 17,000 tons, 19,500 tons and 4500 tons per year. The calculated annual consumption of binders (cement, bitumen, and wood tar) and coke fines in cases of charging different types of briquettes is given in Figure 13. In R11, R13 and R15, ~8000 tons of cement will be replaced by an equal amount of bitumen and wood tar, respectively. In R13 and R15, ~19,000 tons of coke fines will be annually recycled in the briquettes to the BF. The current price of bitumen is higher than the price of cement, but the expected profits gained from savings of lump coke and limestone and lowering of CO₂ emissions by using the developed briquettes might compensate for this difference. However, a cost assessment for the developed briquettes and an analysis of the potential benefits from its utilization in the BF is recommended in the future work.

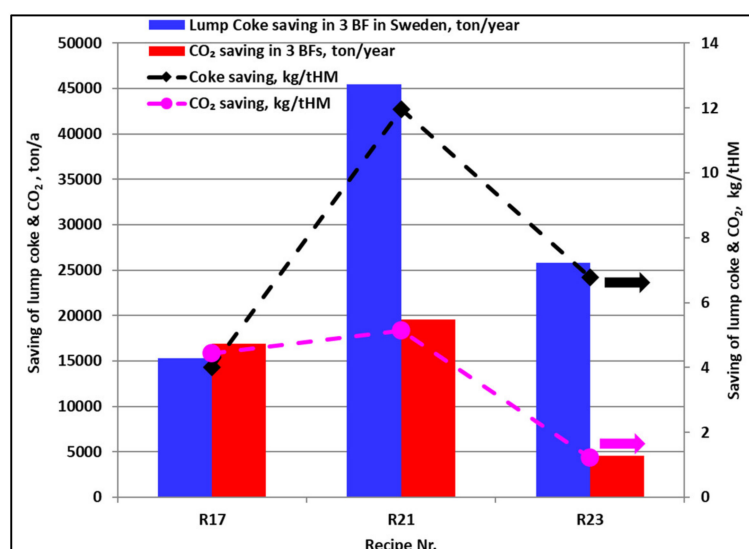


Figure 12. Coke and CO₂ saving by charging developed briquettes.

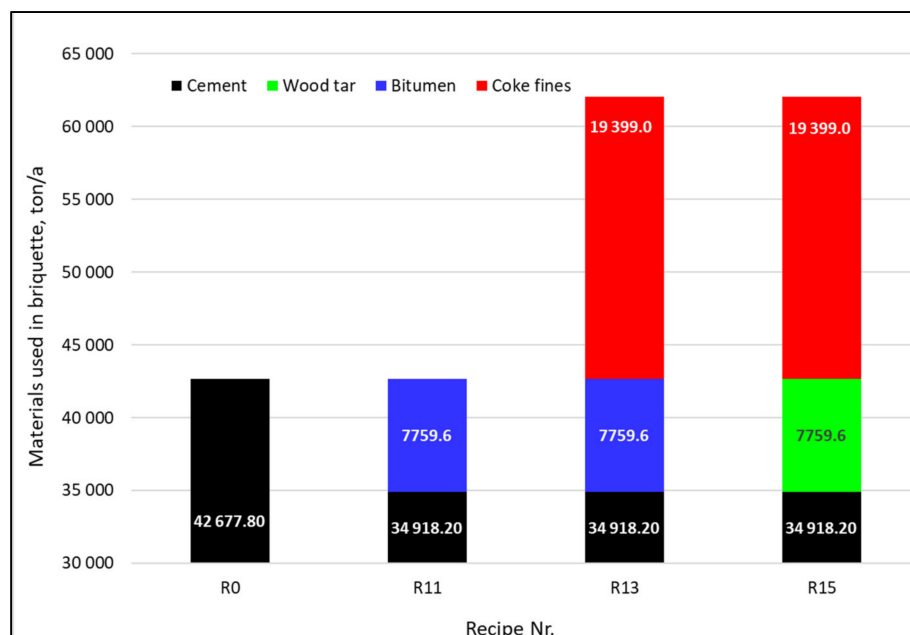


Figure 13. Annual consumption of binders and coke fines in developed briquettes.

4. Conclusions

In this study, organic binders (molasses/lime, bitumen, keracoal, carboxymethyl cellulose and wood tar) were applied for partial replacement of cement in blast furnace (BF) briquettes. Technical-scale briquettes have been developed under simulated industrial conditions using a Vibro press. A reference recipe with traditional cement as the binder and 15 recipes with organic binders were designed and evaluated in terms of mechanical strength and reduction behaviour. A static heat and mass balance model was used to evaluate the impact of developed briquettes on the BF's performance. Based on the results, the following conclusions can be drawn:

1. Among all tested organic binders, bitumen showed cement had equal efficiency with 2 wt.% addition to the briquettes, which replaced 18.2 wt.% of the cement. The other types of organic binders deteriorated the mechanical strength of the briquettes, even at 2 wt.% addition.
2. The briquettes with bitumen showed a higher reduction rate compared to the standard briquettes.
3. The developed briquettes have the potential for annual savings of 15,000–45,000 tons of coke and 4500–19,500 tons of CO₂ emission from the three BFs in Sweden at a full production rate.
4. Approximately 19,000 tons of coke fines can be annually recycled in three BFs in the form of the developed briquettes and this can contribute to savings equal to the amount of lump coke.
5. The annual consumption of limestone at the three BFs can be decreased by 5000–20,000 tons, which contributes to further a reduction in CO₂ emissions.

On the basis of the promising findings presented in this paper, we will continue to study the binding mechanism and test more binders, especially the recently developed innovative organic binders, to enhance the recycling of residues in steel plants.

Author Contributions: E.M.: Conceptualization, methodology, investigation, formal analysis, project administration, writing—original manuscript, review and editing. H.A.: Investigation, formal analysis, writing—review and editing. D.S.: Conceptualization methodology, formal analysis, review and editing. All authors have read and agreed to the published version of the manuscript.

Funding: The research was funded by Vinnova for the InnoBind project grant number (dnr. 2017-05449) and by Formas to InnoAgglo project grant number (2020-02089).

Institutional Review Board Statement: Not applicable.

Informed Consent Statement: Not applicable.

Data Availability Statement: Not applicable.

Acknowledgments: The authors highly appreciate the excellent support provided by SSAB EMEA AB in Luleå for this work and acknowledge the helpful discussions with Anita Wedholm (formerly at SSAB) and Lena Sundqvist Ökvist (Swerim AB) during the project. This work has been carried out within the context of CAMM² (Center of Advanced Mining and Metallurgy) at Luleå University of Technology.

Conflicts of Interest: The authors declare that they have no known competing financial interests or personal relationships that could have appeared to influence the work reported in this paper.

References

1. Fact Sheet-Steel Industry By-Products. Available online: https://www.worldsteel.org/en/dam/jcr:1b916a6d-06fd-4e84-b35d-c1d911d18df4/Fact_By-products_2016.pdf (accessed on 18 January 2018).
2. Schwelberger, J.; Wimmer, G.; Brunner, C.; Fleischander, A. Innovative solutions for recycling of by-products. In Proceedings of the 46th Steelmaking, Rio de Janeiro, Brazil, 17–21 August 2015.
3. Mousa, E.A.; Ahmed, H.M.; Wang, C. Novel approach towards biomass lignin utilization in ironmaking blast furnace. *ISIJ Int.* **2017**, *57*, 1788–1796. [[CrossRef](#)]
4. Wang, C.; Larsson, M.; Lövgren, J.; Nilsson, L.; Mellin, P.; Yang, W.; Salman, H.; Hultgren, A. Injection of solid biomass products into the blast furnace and its potential effects on an integrated steel plant. *Energy Procedia* **2014**, *61*, 2184–2187. [[CrossRef](#)]
5. Pach, M.; Zanzi, R.; Björnbom, E. Torrefied biomass a substitute for wood and charcoal. In Proceedings of the 6th Asia-Pacific International Symposium on Combustion and Energy Utilization, Kuala Lumpur, Malaysia, 20–22 May 2002.
6. Ribeiro, J.M.C.; Godina, R.; de Oliveira Matias, J.C.; Nunes, L.J.R. Future perspectives of biomass torrefaction: Review of the current state-of-the art and research development. *Sustainability* **2018**, *10*, 2323. [[CrossRef](#)]
7. Gudenau, H.W.; Senk, D.; Wang, S.; De Melo Martins, K.; Stephany, C. Research in the reduction of iron ore agglomerates including coal and C-containing dust. *ISIJ Int.* **2005**, *45*, 603–608. [[CrossRef](#)]
8. Ueda, S.; Yanagiya, K.; Watanabe, K.; Murakami, T.; Inoue, R.; Ariyama, T. Improvement of reactivity of carbon iron ore composite with biomass char for blast furnace. *ISIJ Int.* **2009**, *49*, 1505–1512. [[CrossRef](#)]
9. Kundvist, K.; Brämning, M.; Riesbeck, J.; Wedholm, A. New methods for waste minimization in an integrated steel site. *Chem. Eng. Trans.* **2015**, *45*, 739–744.
10. Robinson, R.; Sundqvist, L. Recycling of by-product pellets as burden in the blast furnace process: A lab and pilot scale investigation. *Steel Res.* **2004**, *75*, 99–105. [[CrossRef](#)]
11. Sundqvist, L.; Jonsson, K.O.; Lampinen, H.O.; Eriksson, L.E. Recycling of in-plant fines as cold bonded agglomerates. In *Committee on Raw Materials-Seminar Proceeding*; International Iron and Steel Institute (IISI): Brussels, Belgium, 1999; pp. 44–60.
12. Singh, M.; Björkman, B. Swelling behaviour of cement-bonded briquettes-proposed model. *ISIJ Int.* **2004**, *44*, 482–491. [[CrossRef](#)]
13. Singh, M. Studies on the Cement-Bonded Briquettes of Iron and Steel Plant By-Products as Burden Material for Blast Furnaces. Ph.D. Thesis, Department of Chemical and Metallurgical Engineering, Division of Process Metallurgy, Luleå University of Technology, Luleå, Sweden, 2003.
14. Tanaka, Y.; Ueno, T.; Okumura, K.; Hayashi, S. Reaction behavior of coal rich composite iron ore hot briquettes under load at high temperatures until 1400 °C. *ISIJ Int.* **2011**, *51*, 1240–1246. [[CrossRef](#)]
15. Kasai, A.; Matsui, Y. Lowering thermal reserve zone temperature in blast furnace by adjoining carbonaceous materials and iron ore. *ISIJ Int.* **2004**, *44*, 2073–2078. [[CrossRef](#)]
16. Ujisawa, Y.; Nakano, K.; Matsukura, Y.; Sunahara, K.; Komatsu, S.; Yamamoto, T. Subjects for achievement of blast furnace operation with low reducing agent rate. *ISIJ Int.* **2005**, *45*, 1379–1385. [[CrossRef](#)]
17. Mousa, E.A.; Lundgren, M.; Ökvist, L.S.; From, L.-E.; Robles, A.; Hällsten, S.; Sundelin, B.; Friberg, H.; El-Tawil, A. Reduced carbon consumption and CO₂ emission at the blast furnace by use of briquette containing torrefied sawdust. *J. Sustain. Metall.* **2019**, *5*, 391–401. [[CrossRef](#)]
18. Mousa, E.A.; Ahmed, H.M. *Utilization of biomass as an alternative fuel in iron and steel making*, In *Iron Ore Textbook, Mineralogy, Processing and Environmental Sustainability*, 2nd ed.; Woodhead Publishing Series in Metals and Surface Engineering; Elsevier: Amsterdam, The Netherlands, 2021; pp. 665–690.
19. Mousa, E.; Kazemi, M.; Larsson, M.; Karlsson, G.; Persson, E. Potential for developing biocarbon briquettes for foundry industry. *Appl. Sci.* **2019**, *9*, 5288. [[CrossRef](#)]
20. Rist, A.; Bonnavard, G. Rduction d'un lit d'oxydes de fer par un gaz. *Rev. Métallurgie* **1963**, *60*, 23–37. [[CrossRef](#)]

21. Geerdes, M.; Chaigneau, R.; Lingardi, O. *Modern Blast Furnace Ironmaking: An Introduction*; IOS Press: Amsterdam, The Netherlands, 2020.
22. Ahmed, H.; Viswanathan, N.N.; Bjorkman, B. Isothermal reduction kinetics of self-reducing mixtures. *Ironmak. Steelmak.* **2017**, *44*, 66–75. [[CrossRef](#)]
23. Hoey, P.L.; Bodén, A.; Wang, C.; Grip, C.-E.; Jansson, P. Design and application of a spread sheet-based model of the blast furnace factory. *ISIJ Int.* **2010**, *50*, 924–930. [[CrossRef](#)]